Silicon (2018) 10:403–411
DOI 10.1007/s12633-016-9462-4

ORIGINAL PAPER

A Self-Powered Heterojunction Photodetector Based on a PbS Nanostructure Grown on Porous Silicon Substrate

Z. A. Bashkany[1] · Ismail Khalaf Abbas[1] · M. A. Mahdi[2] · H. F. Al-Taay[3] · P. Jennings[4]

Received: 19 December 2015 / Accepted: 12 August 2016 / Published online: 28 October 2016

Abstract A photosensor was fabricated based on a lead sulfide (PbS)/porous silicon (Ps) heterojunction. An n-type Si(100) single crystal wafer was used to prepare the Ps using a photo-electrochemical etching method. A PbS nanocrystalline thin film was deposited onto the Ps substrate using a microwave-assisted chemical bath deposition (MA-CBD) technique. The current-voltage (I-V) characteristics of the fabricated PbS/Ps photosensor were studied under dark, 10 mW/cm^2, 20 mW/cm^2, and 40 mW/cm^2 illumination by light. The device shows good response to light even without a bias voltage and the sensitivity when the applied voltage is 0 V decreased from 5.66×10^4 % under 10 mW/cm^2 to 1.8×10^3 % when the device is illuminated by 40 mW/cm^2 intensity light. The fabricated PbS/Ps photdetector shows a faster response to light of 0.43 sec when the applied voltage and intensity of light were 1.0 V and 40 mW/cm^2, respectively. Moreover, the fastest fall time was 0.4 sec obtained for the device that was exposed to 40 mW/cm^2 light and biased by 0.75 V.

✉ M. A. Mahdi
mazinauny74@yahoo.com

[1] Physics Department, College of Science, Mosul University, Mosul, Iraq

[2] Basrah Nanomaterials Research Group (BNRG), Department of Physics, College of Science, University of Basrah, Basrah, Iraq

[3] Department of Physics, College of Science for Women, University of Baghdad, Baghdad, Iraq

[4] School of Engineering and Information Technology, Murdoch University, South St., Murdoch, WA 6150, Australia

Keywords Photosensor · Porous silicon · PbS · Nanotechnology

1 Introduction

At the nanometer sized scale, a gradual transition from the solid state (bulk) to molecular structure occurs as the particle size decreases. In this very small size regime, the physical and chemical properties of the particles strongly depend on their size [1–5]. Thus, fabrication strategies for low dimensional nanostructures such as nanocrystals, nanoparticles, nanowires, etc. have attracted a lot of attention [6–8]. Nanocrstallites, especially semiconductors, such as silicon (Si) and lead sulfide (PbS), have attracted a lot of interest because of their unique physical and chemical properties [9, 10]. Porous silicon (Ps) has attracted much attention for optoelectronic devices in recent years, especially after the discovery of its effective visible photoluminescence (PL) and visible electroluminescence (EL) [11, 12]. There are additional characteristics that led to this attention, such as a direct and wide modulated energy band gap, high resistivity, the same single-crystal structure as bulk Si [13], its widely different structures (macro, meso and micro) having a very large surface area to volume ratio [14, 15], simple and inexpensive fabrication and its compatibility with current silicon microelectronic processing [16]. These advantages make it a suitable material for photodetectors [17].

On the other hand, lead sulfide (PbS), which is an important binary IV–VI semiconductor material with a direct narrow optical energy gap of 0.41 eV at 300 K, has been intensively studied as a unique semiconductor material. PbS nanocrystals are of interest because of their strong quantum confinement, due to the large exciton Bohr radius of both

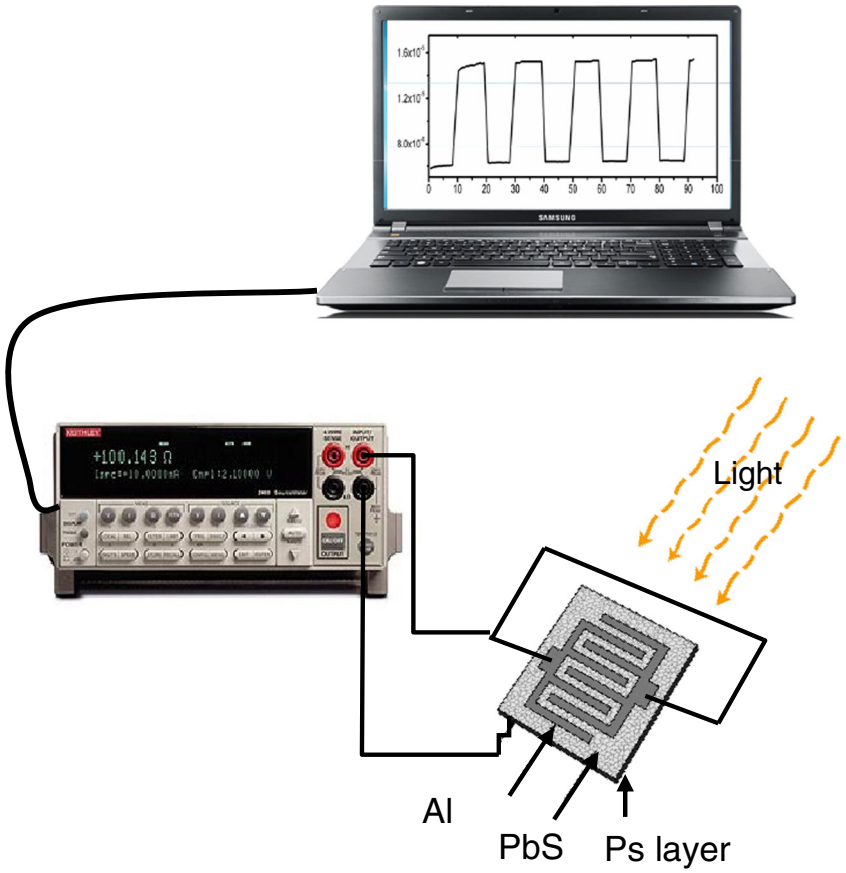

Fig. 1 Schematic diagram of the fabricated photosensor and the system of test

electrons and holes (18 nm) [18–20]. Therefore, PbS can be utilized for designing multi-element galvanomagnetic, thermoelectric and optoelectronic (in IR region) sensors for recording various physical fields with high spatial and temporal resolution [21]. It is of importance to produce PbS thin films on silicon substrates because this provides a means for integration of the thin film optoelectronic structure into electronic devices formed on silicon substrates. Unfortunately, direct epitaxial growth of IV–VI compound semiconductors on silicon substrates has been a problem. However, the 6.2–9.4 % mismatch of the lattice constants and ∼1000 % difference in thermal expansion coefficients prohibit deposition growth of IV-VI materials on silicon. Employing either buffer layers with variable lattice constant [22] or stressed superlattices [23] can eliminate the problem. However, the production of multilayer structures is complex, poorly compatible with conventional silicon technology and expensive equipment is needed [21]. Porous silicon has been utilized as a buffer between a Si substrate and a growing film such as GaAsS [24], diamond [25], and PbTe [26]. The porous silicon (Ps) buffer layer allows the implantation of lattice-mismatched hetero-epitaxial films on Si substrates [27].

The present work is aimed at fabricating a c-nSi/pSi/PbS heterostructure photodetector (PD). The microwave-assisted CBD method was used to prepare the p-PbS layer on a n-Ps substrate. The prepared films were characterized by X-ray diffraction and scanning electron microscopy. The optical properties were also studied. The performance of the fabricated PD was investigated through (I–V) and photo-response measurements.

2 Experimental Details

2.1 Preparation of the Porous Silicon Layer

An n-type silicon wafer of (100) orientation, (1–10 Ωcm) resistivity and 380 μm thickness was used to grow the porous silicon substrate. The wafer was cut into square pieces with dimensions of 1.4 cm × 1.4 cm. The wafer surface was cleaned ultrasonically with isopropanol, methanol and acetone, respectively. Then the samples were immersed in 10 % hydrofluoric acid (HF) solution for 30 sec to remove the native oxide layer and then washed with deionized water.

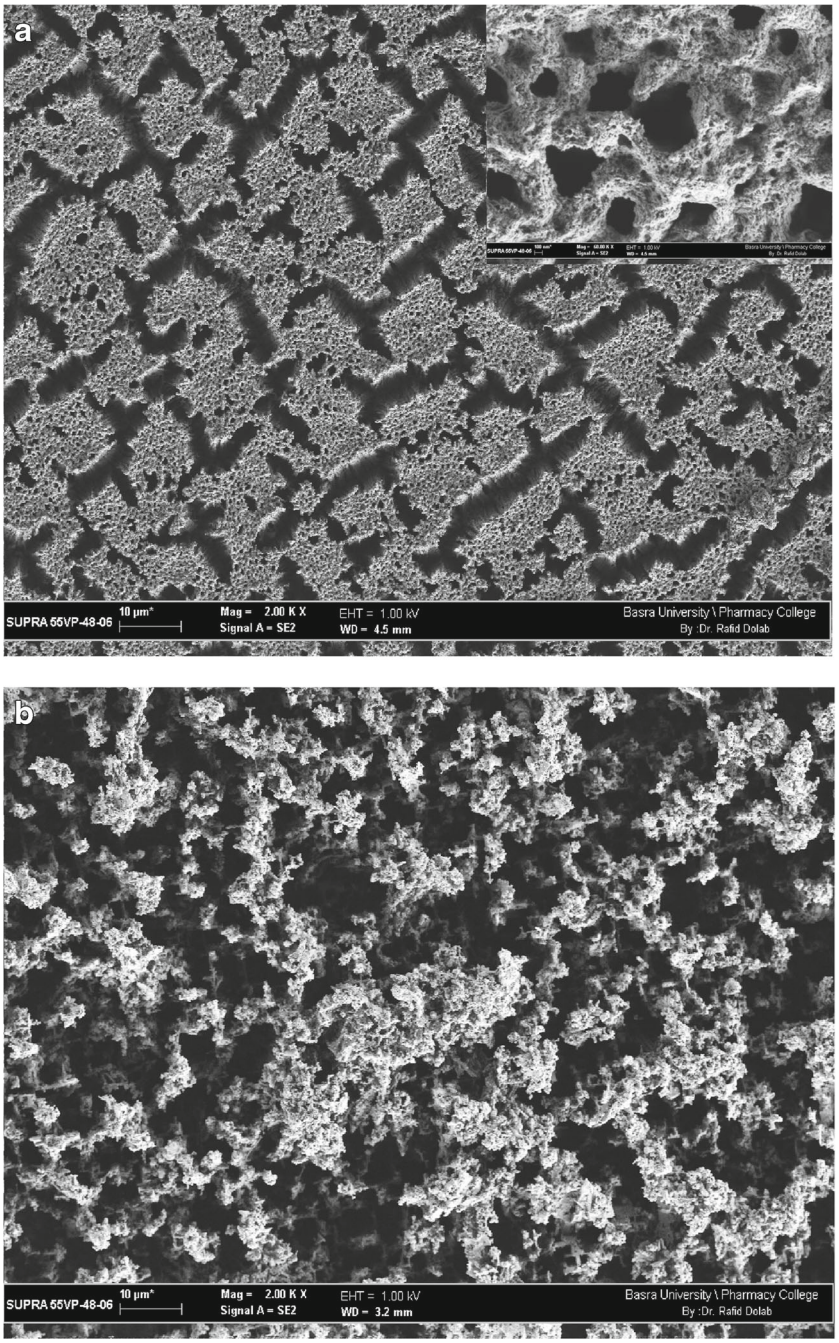

Fig. 2 SEM images of **a** porous silicon substrate, and **b** PbS nanocrystalline thin film onto Ps substrate

The porous silicon samples were prepared by a photo-electrochemical etching process. A cell was mounted on Teflon, which is resistive to attack from the HF electrolyte. The silicon wafer serves as the anode whereas the cathode is connected to a platinum (Pt) wire that is submerged in the HF electrolyte. The electrochemical process is carried out under constant current density of 25 mA/cm^2 for 15 min and a concentration of 50 % HF, 99.90 % ethanol (HF:C_2H_5OH) with a volume ratio of 1:3. The surface of the Si wafer was illuminated by a 38 mW/cm^2, 532 nm green laser beam during the preparation process. Finally, the manufactured porous silicon sample was washed in distilled water and left to dry naturally.

2.2 Preparation of PbS Nanocrystalline Thin Films

The deposition was performed in a reactive solution prepared in a 50 ml beaker containing 0.1M of both lead nitrate [$Pb(NO_3)_2$] and thiourea [CH_4N_2S (TU)]. The pH of the solution was fixed at 12 by adding a few drops of sodium

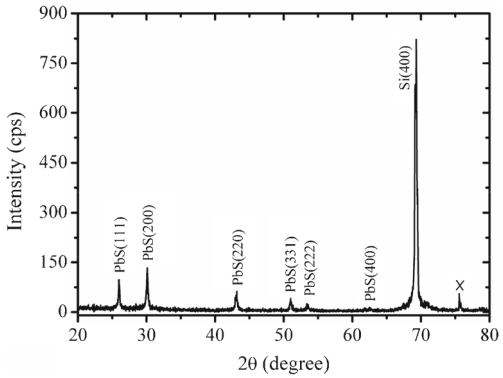

Fig. 3 XRD pattern of PbS nanocrystalline thin film prepared onto Ps substrate

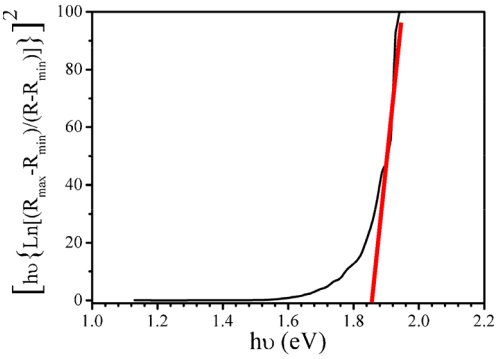

Fig. 5 Optical band gap of the prepared PbS nanocrystalline thin film onto Ps substrate

hydroxide (NaOH), and the total volume was completed by adding water to 100 ml. Then the freshly prepared porous silicon was fixed vertically in the chemical bath and the beaker was placed in the microwave oven system (2.4 GHz) at 65–70 °C for 45 min. For the first 5 min of reaction time, the solution remained transparent, indicating the occurrence of decomposition reactions. Beyond 5 min, the color of the solution turned dark grey, indicating the formation of PbS compound. Finally, the sample was removed from the solution and washed by hot distilled water and left to dry in air. To increase the thickness of the PbS thin film, the preparation process was repeated once again under the same conditions. The schematic diagram for the fabrication of the photodetector is shown in Fig. 1.

3 Results and Discussion

3.1 Surface Morphology

Figure 2a shows the FE-SEM micrograph of the prepared Ps. The pores are distributed over the whole surface of the sample. Large pores are apparent with inner diameters ranging from (250–700 nm) as shown in Fig. 2a. However, there are also many pores with smaller diameters spread over the surface of the Ps. Figure 2b shows the FE-SEM image of the PbS nanocrystalline thin film prepared on the Ps substrate by the MA-CBD method. The PbS is grown on the rims of the larger pores and forms an arboreal structure. However, porous materials can be used to synthesize various types of PbS semiconductor. Gao et al. [28] obtained PbS nanoparticles and nanowires structure when they used mesoporous silica as a substrate to prepare uniform PbS nanostructures by a chemical method.

3.2 Crystalline Structure

Figure 3 shows the XRD pattern of the PbS nanocrystalline thin film grown on a porous silicon substrate The diffraction peaks appeared at diffraction angles (2θ) of 25.95, 30.08, 43.09, 51.01, 53.46, and 62.56 degrees, corresponding to the (111), (200), (220) (311), (222) and (400) planes of the cubic rock salt (NaCl) type structure of PbS,

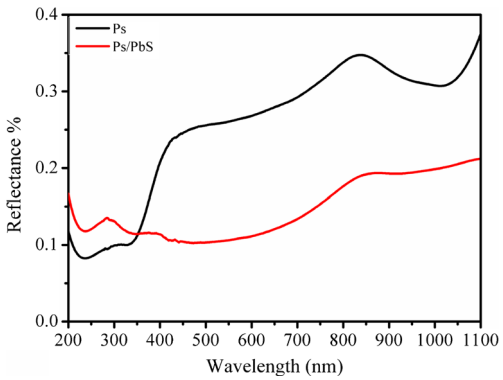

Fig. 4 Reflectance spectra of porous silicon substrate and PbS nanocrystalline thin film onto Ps substrate

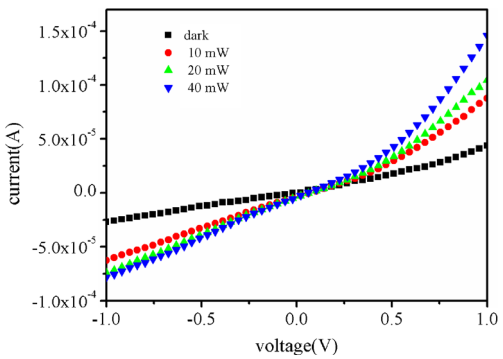

Fig. 6 I-V characteristic of PbS/Ps photosensor under various powers of light

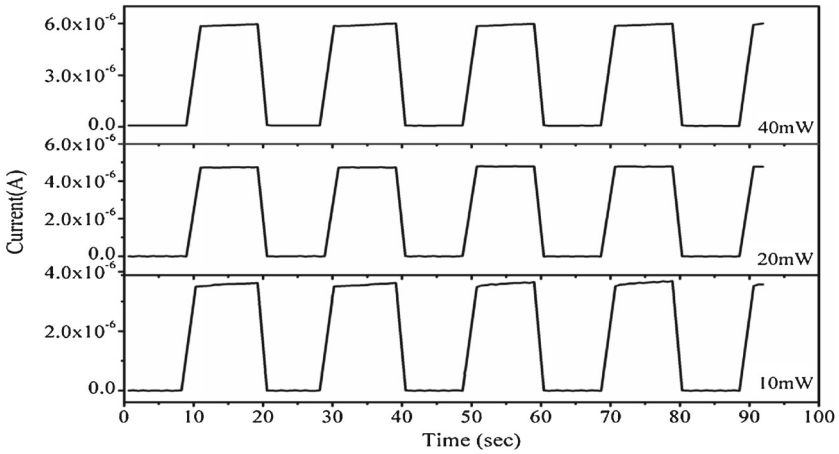

Fig. 7 Photoresponse of PbS/Ps photosensor illuminated by various chopped light at 0 V bias voltage

respectively, according to the standard database (ICDD, PDF-4, 03-066-00243). The sharp peak at 2θ of 69.34° is related to the (400) plane of the silicon diamond structure. The lattice constant a of the cubic unit cell is calculated [29] and found to be 5.94 Å and it is close to the standard value of 5.93 Å for PbS. The average particle size P_s was estimated [30] and the average value of the PbS thin films for the planes (111), (200), and (311), is 66 nm.

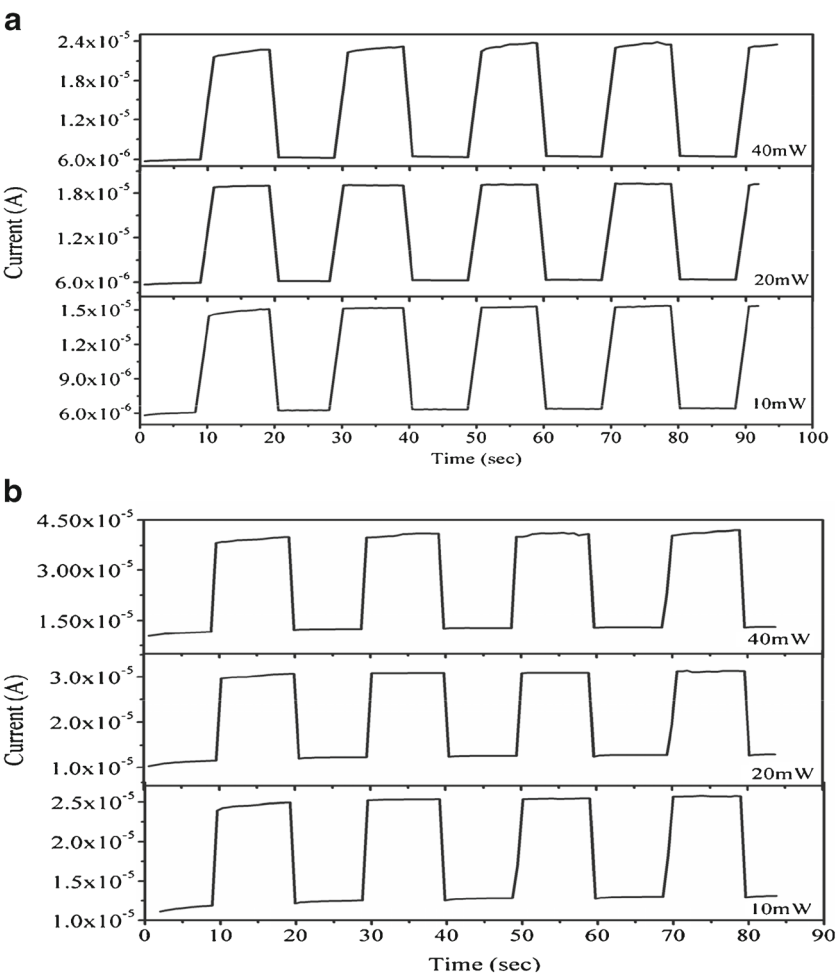

Fig. 8 Photoresponse of PbS/Ps photosensor illuminated by various chopped light at bias voltage of **a** 0.25V and **b** 0.5 V

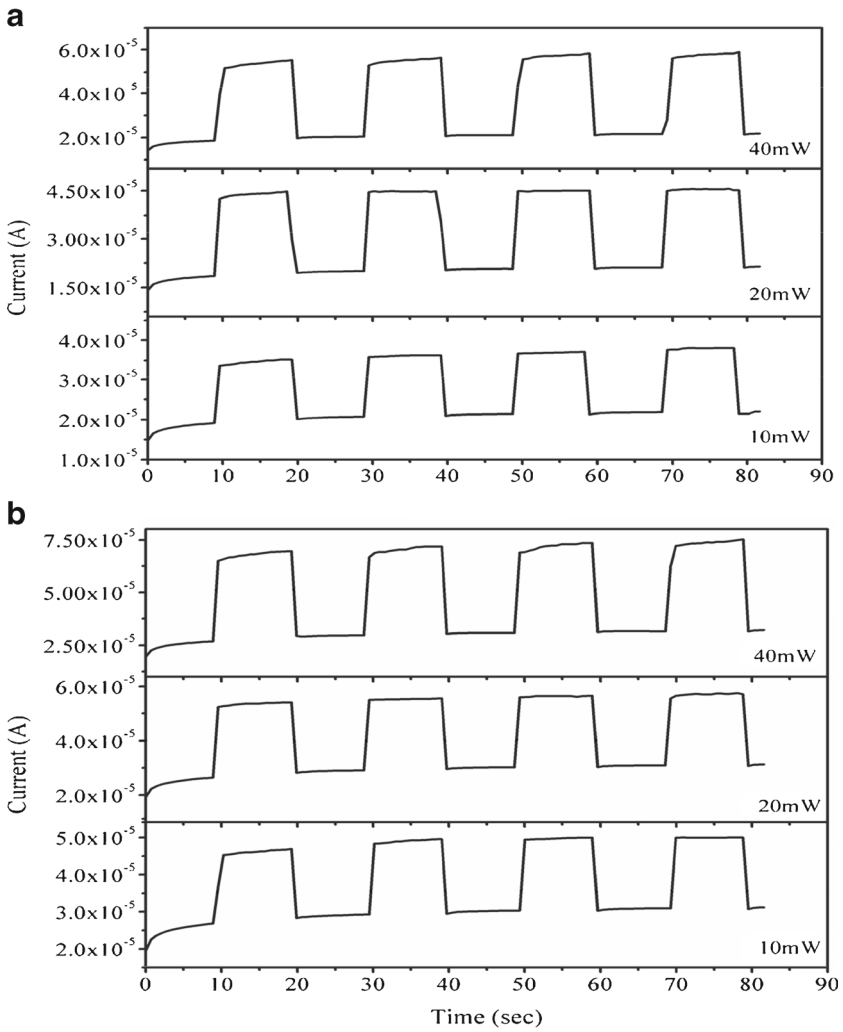

Fig. 9 Photoresponse of PbS/Ps photosensor illuminated by various chopped light at bias voltage of **a** 0.75V and **b** 1.0 V

Gertman et al. [31] found that the growth mechanism and the particles size of PbS thin films prepared by the CBD method on ZnO NWs are affected by the concentration of thiourea and temperature of growth.

3.3 Optical Properties

3.3.1 Reflectance

Figure 4 shows the reflectance spectra of the Ps layer and the PbS/Ps structure. The Ps substrate shows a very low value (less than 0.4 %) of light reflectance in the UV and visible region of the electromagnetic spectrum. However, the deposition of the PbS nanocrystalline thin film onto the Ps substrate also led to a decrease in light reflectance to less than 0.2 %. It is known that surface roughness has a great effect on the optical measurements, mainly at energies close to electronic transitions [32]. In addition, reflectance measurements can be used to determine the optical band gaps of semiconductor thin films [33]:

The optical band gap can be estimated from a plot of hυ (abscissa) and the square of $\ln[h\upsilon(R_{\max} - R_{\min})/(R - R_{\min})]$ as shown in Fig. 5. The calculated optical band gap

Table 1 Dependence of the photocurrent for the PbS/Ps photosensor on the bias voltage and light intensity

Bias (V)	Dark I (μA)	10 mW I_{ph} (μA)	20 mW I_{ph} (μA)	40 mW I_{ph} (μA)
0	9.7×10^{-6}	3.6	4.7	5.5
0.25	6.4	15.2	19	23
0.50	12.7	25	30	41
0.75	21.2	38	45	58
1.0	30.8	49.8	56	73

Table 2 Dependence of the rise and fall times and the device sensitivity on the light intensity and bias voltage

Bias	10 mW			20 mW			40 mW		
(V)	Rt (sec)	Ft (sec)	S%	Rt (sec)	Ft (sec)	S%	Rt (sec)	Ft (sec)	S%
0	1.6	1.13	566×10^2	1.6	1.1	386×10^2	1.49	1.02	18×10^2
0.25	1.5	1.08	139	1.57	0.97	22	1.66	1.06	27
0.50	0.54	0.54	98	0.53	0.54	15	0.55	0.53	22
0.75	0.53	0.58	73	0.52	0.43	14	0.58	0.4	16
1.0	0.52	0.54	62	0.45	0.51	88	0.43	0.53	13

of the PbS was 1.85 eV and this value is much higher than the band gap of bulk PbS (~0.41 eV). Obaid et al. [34] studied the effect of different deposition times on the optical band gap of PbS nanocrystalline thin films prepared via the microwave assisted CBD method and they found that the values ranged from 1.6 eV to 2.75 eV.

3.4 Photoelectrical Properties

Figure 6 shows the I-V characteristic of the fabricated PbS/Ps photosensor under dark, 10 mW/cm^2, 20 mW/cm^2 and 40 mW/cm^2 light intensity. In the dark case, the current flowing at a low voltage corresponds to that typical of thermionic emission. However, the device shows nonlinear behavior and the current increased as the applied voltage and intensity of light are increased. The resistance of the device at applied bias of 1.0 V decreases from 32.4 kΩ in the dark to 13.7 kΩ when the device is illuminated by light intensity of 40 mW/cm^2. It is clear that when the device is illuminated by light, a photocurrent is produced due to generation of electron-hole pairs. The fabricated photosensor is strongly affected by the parameters of the preparation. For example, Naderi and Hashim [35] discovered that the photocurrent of the MSM photosensor prepared based on Al/PS is increased when the current density of the preparation Ps is increased. Rossi and Bohn [36] found that the responsivity of a Al/PS photosensor is about 2.5 A/W when the device is exposed to 400 nm light and rises to 5.5 A/W at 800 nm.

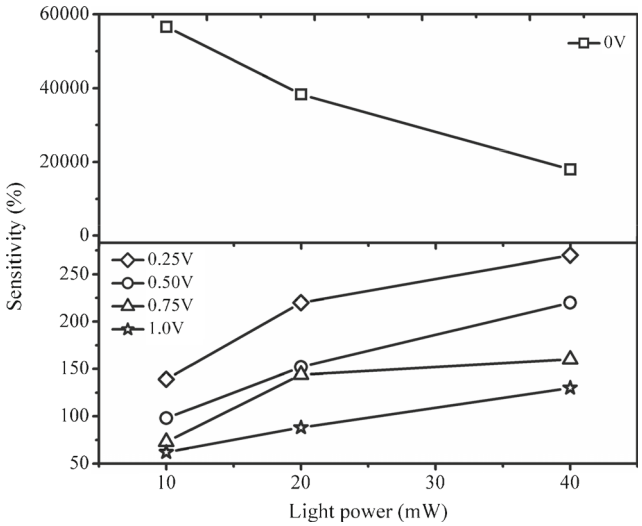

Fig. 10 Photosensitivity of PbS/Ps photosensor illuminated by various powers of light at different biases voltage

The photocurrent response of the fabricated device was investigated under various bias voltages and light intensity. Figure 7 shows the photocurrent response of the device biased by 0 V under 10, 20, and 40 mW light intensity. In all cases, the current increased to the saturation value when the sample was illuminated and decreased again when the light was switched off. However, the device shows good response to light even without bias voltage as a result of the photovoltaic effect of the p-n junction.

Figures 8 and 9 show the photoresponse of the PbS/Ps photosensor under bias voltages of 0.25–1.0 V when the device was illuminated by 10, 20, and 40 mW/cm^2 intensity. The photocurrent value was found to depend on the bias voltage as well as the intensity of light values. For example, under 0 V bias, we found that the photocurrent increased from 9.7×10^{-6} μA to 5.5 μA when the device was exposed to 40 mW, while the photocurrent increased from 30.8 μA in the dark to 73 μA under 40 mW/cm^2 when the bias voltage was 1.0 V (see Table 1).

The speed of photoresponse is one of the important parameters of the photosensor. Rise time (Rt) is the time to increase the photocurrent from 10 to 90 % of the saturation value while the fall time (Ft) is the time to decrease the photocurrent from 90 to 10 % of the saturation value.

Under 0 V bias, the PbS/Ps photosensor Rt was 1.6, 1.1, and 1.45 sec when the device was illuminated by 10, 20, and 40 mW/cm^2 intensity light, respectively. Also, the Ft value was around 1.0 sec when the sensor was illuminated by different intensities of light. The PbS/Ps photosensor was faster when the device was under bias voltage more than 0 V. The fastest Rt was 0.43 sec when the device was illuminated by 40 mW/cm^2 under 1V bias, while the fastest recovery time was 0.4 sec for the sensor under 40 mW and 0.75 V (see Table 2). Rajabi et al. [37] fabricated ZnO nanowire/Ps photosensors and they found that the rise and decay time were 19 sec, and 62 sec, respectively when the device is used to detect 325 nm UV light under reverse bias of 5 V.

The photosensitivity of the fabricated device at a different applied bias voltage was also determined [38]. The device under 0 V bias shows high sensitivity to the light compared with the other values of bias. The sensitivity of the fabricated Pbs/Ps photosensor biased by 0 V decreased from 5.66×10^4 % under 10 mW/cm^2 to 1.8×10^3 % when the device is illuminated by 40 mW/cm^2 light intensity. However, the decreasing sensitivity value of the devices at 0 V bias, as the intensity of the light was increased could be due to an increase in the temperature of the device. This produces a current (thermocurrent) that counters the photocurrent, resulting in a reduction in its value. The photosensitivity of the fabricated sensor increased when the intensity of the light increased from 10 to 40 mW/cm^2 in all cases for the devices under various bias voltages as shown in Fig. 10.

4 Conclusions

We report, for the first time, to our knowledge, a self-powered white light photodetector based on a PbS/Ps heterojunction. Porous silicon is a suitable substrate that can be used to prepare nanocrystalline thin films for optoelectronics applications. There are two very significant advantages of using porous silicon to prepare photosensors. They are the very high surface to volume ratio that leads to increased exposed area to light and the direct optical band gap of Si.

The PbS/Ps photosensor was fabricated for white light sensing under various intensities of light and applied voltage. The sensor shows very high sensitivity to light when the bias voltage is 0 V because of the photovoltaic effect of the PbS/Ps heterojunction device. We found that the response of the fabricated photosensor to light was affected by the intensity of light illumination and bias voltage. The PbS/Ps device had its fastest response under high intensity of light (40 mW/cm^2) and an applied voltage of 1.0 V. From the results obtained we can conclude that fabrication of a self-intensified photosensor, based on a nanocrystalline semiconductor/porous silicon hetrojunction is a promising way to get a high photoresponse speed and high light sensitivity.

References

1. Brus L (1986) Electronic wave functions in semiconductor clusters: experiment and theory. J Phys Chem 90:2555–2560
2. Henglein A (1989) Small-particle research: physicochemical properties of extremely small colloidal metal and semiconductor particles. Chem Rev 89:1861–1873
3. Wang Y, Herron N (1991) Nanometer-sized semiconductor clusters: materials synthesis, quantum size effects, and photophysical properties. J Phys Chem 95:525–532
4. Weller H (1993) Colloidal semiconductor Q-particles: chemistry in the transition region between solid state and molecules. Angew Chem Int Ed Engl 32:41–53
5. Mahdi MA, Hassan JJ, Hassan Z, Ng SS (2012) Growth and characterization of ZnxCd1 xS nanoflowers by microwave-assisted chemical bath deposition. J Alloys Compd 541:227–233
6. Xia Y, Mokaya R (2004) Synthesis of ordered mesoporous carbon and nitrogen-doped carbon materials with graphitic pore walls via a simple chemical vapor deposition method. Adv Mater 16:1553–1558
7. Rao C, Deepak FL, Gundiah G, Govindaraj A (2003) Inorganic nanowires. Prog Solid State Chem 31:5–147
8. Al-Taay HF, Mahdi MA, Parlevliet D, Hassan Z, Jennings P (2014) Growth and characterization of silicon nanowires catalyzed by Zn metal via pulsed plasma- enhanced chemical vapor deposition. Superlattice Microst 68:90–100
9. Liu X, Zhang M (2000) Studies on PBS and PBSE detectors for IR system. Int J Infrared Millimeter Waves 21:1697–1701
10. Patil R, Pathan H, Gujar T, Lokhande C (2006) Characterization of chemically deposited nanocrystalline PbS thin films. J Mater Sci 41:5723–5725
11. Canham L (1990) Silicon quantum wire array fabrication by electrochemical and chemical dissolution of wafers. Appl Phys Lett 57:1046–1048
12. Koshida N, Koyama H (1992) Visible electroluminescence from porous silicon. Appl Phys Lett 60:347–349
13. Lee M.-K., Chu C.-H., Wang Y.-H., Sze S (2001) 1.55-μm and infrared-band photoresponsivity of a Schottky barrier porous silicon photodetector. Opt Lett 26:160–162
14. Fauchet P, Von Behren J, Hirschman K, Tsybeskov L, Duttagupta S (1998) Porous silicon physics and device applications: a status report. Phys Status Solidi (A) 165:3–13
15. Herino R, Bomchil G, Barla K, Bertrand C, Ginoux J (1987) Porosity and pore size distributions of porous silicon layers. J Electrochem Soc 134:1994–2000
16. Lopez HA (2001) Porous silicon nanocomposites for optoelectronic and telecommunication applications in University of Rochester
17. Hadi H, Ismail R, Habubi N (2014) Optoelectronic properties of porous silicon heterojunction photodetector. Indian J Phys 88:59–63
18. Martin P, Netterfield R, Sainty W (1982) Spectrally selective PbS films produced by ion beam sputtering. Thin Solid Films 87:203–206
19. Hines MA, Scholes GD (2003) Colloidal PbS nanocrystals with size-tunable near-infrared emission: observation of

post-synthesis self-narrowing of the particle size distribution. Adv Mater 15:1844–1849
20. Chen Q, Zhou G, Zhu J, Fan C, Li X-G, Zhang Y (1996) Ultraviolet light emission from porous silicon hydrothermally prepared. Phys Lett A 224:133–136
21. Yakovtseva V, Vorozov N, Dolgyi L, Levchenko V, Postnova L, Balucani M, Bondarenko V, Lamedica G, Ferrara V, Ferrari A (2000) Porous silicon: a buffer layer for PbS heteroepitaxy. Physica Status Solidi Applid Research 182:195–200
22. Zogg H, Blunier S, Fach A, Maissen C, Müller P., Teodoropol S, Meyer V, Kostorz G, Dommann A, Richmond T (1994) Thermal-mismatch-strain relaxation in epitaxial CaF 2, BaF 2/CaF 2, and PbSe/BaF 2/CaF 2 layers on Si (111) after many temperature cycles. Phys Rev B 50:10801–10810
23. Wada M, Seko M, Sekiguchi Y, Iwaoka H (1993) Avalanche photodiode with AliNAsP cap layer, in Google Patents
24. Borisenko V, Filonov A, Gaponenko S, Gurin V (1999) Physics, chemistry and application of nanostructures, World Scientific
25. Raiko V, Spitzl R, Engemann J, Borisenko V, Bondarenko V (1996) MPCVD Diamond deposition on porous silicon pretreated with the bias method. Diam Relat Mater 5:1063–1069
26. Belyakov L, Zakharova I, Zubkova T, Musikhin S, Rykov S (1997) Study of PbTe photodiodes on a buffer sublayer of porous silicon. Semiconductors 31:76–77
27. Luryi S, Suhir E (1986) New approach to the high quality epitaxial growth of lattice-mismatched materials. Appl Phys Lett 49:140–142
28. Gao F, Lu Q, Liu X, Yan Y, Zhao D (2001) Controlled synthesis of semiconductor PbS nanocrystals and nanowires inside mesoporous silica SBA-15 phase. Nano Lett 1:743–748
29. Cullity B (1972) Elements of X-Ray Diffraction. Addison-Wesley, Reading USA
30. Mahdi MA, Hassan, Kasim SJ, Ng SS, Hassan Z (2014) Solvothermal growth of single-crystal CdS nanowires. Bull Mater Sci 37:337–345
31. Gertman R, Osherov A, Golanb Y, Fisher IV (2014) Chemical bath deposited PbS thin films on ZnO nanowires for photovoltaic applications. Thin Solid Films 550:149–155
32. Valenzuela-Jauregui JJ, Ramirez-Bon R, Mendoza-Galvan A, Sotelo-Lerma M (2003) Properties of PbS thin films chemically deposited at different Temperatures. Thin Solid Films 441:104–110
33. Kumar V, Sharma SK, Sharma TP, Singh V (1999) Band gap determination in thick lms from reflectance measurements. Opt Mater 12:115–115
34. Obaid A, Mahdi M, Hassan Z, Bououdina M (2012) Characterization of nanocrystalline PbS thin films prepared using microwave-assisted chemical bath deposition. Mater Sci Semicond Process 15:564–571
35. Naderi N, Hashim M (2012) Effect of surface morphology on electrical properties of electrochemically-etched porous silicon photodetectors. Int J Electrochem Sci 7:11512–11515
36. Rossi AM, Bohn HG (2005) Photodetectors from porous silicon. Physica Status Solidi (A):1644–1647
37. Rajabi M, Dariani RS, Iraji Zad A (2012) UV Photodetection of laterally connected ZnO rods grown on porous silicon substrate. Sensors Actuators A 180:11–14
38. Mahdi MA, Hassan JJ, Ahmed NM, Ng SS, Hassan Z (2013) Growth and characterization of CdS single-crystalline micro-rod photodetector. Superlattice Microst 54:137–145